

Finite-Volume Method for the Calculation of Compressible Chemically Reacting Flows

Thomas R.A. Bussing* and Earll M. Murman†

Massachusetts Institute of Technology, Cambridge, Massachusetts

The time-dependent Euler and Navier-Stokes equations including the effects of finite-rate chemistry are numerically integrated forward in time to predict the steady-state behavior of compressible chemically reacting flows. An efficient acceleration technique is developed based on preconditioning the conservation equations. One possible choice for the preconditioner leads to a procedure which is equivalent to treating the convection and diffusion terms explicitly and species source terms implicitly. These methods can be viewed as ways of rescaling the equations in time so that all chemical and convective phenomena evolve on comparable pseudotime scales. For the steady-state solutions in this paper, the number of iterations needed to solve reacting problems is approximately the same as for nonreacting problems. The methods are applied to a quasi-one-dimensional dissociation model problem, a quasi-one-dimensional H_2 -air combustion problem, and to two-dimensional inviscid and viscous premixed H_2 -air problems.

I. Introduction

FLows involving finite-rate chemistry can be described by a set of conservation equations which often can be very difficult to solve numerically because of stiffness. Mathematically speaking, stiffness can be defined by examining the eigenvalues of the Jacobian matrix of the governing equation system. This quantity is formed by differentiating the flux vectors F and G with respect to the state vector U . Stiffness is defined as the ratio of the largest eigenvalue to the smallest eigenvalue. Stiffness can be interpreted in terms of time or length scales. For the remainder of the article, the term stiffness will refer to time scales unless otherwise indicated. A useful definition of stiffness is the ratio of the largest to the smallest time scale,

$$\text{Stiffness} = \tau_{\text{largest}} / \tau_{\text{smallest}} \quad (1)$$

High levels of stiffness can severely degrade the performance of numerical methods, as will be illustrated in this article. For the system of equations governing chemically reacting flows, stiffness typically arises from the source terms H in the species conservation equations. If the source terms are large, they produce rapid temporal and spatial changes in the dependent variables, leading to a range of physical time scales. For problems involving more than one specie, several chemical time scales can occur. In addition, there are fluid dynamic time scales associated with convection and diffusion. For the reacting flows considered in this article the stiffness parameter can be as high as 10^6 .

In 1952, Curtiss and Hirschfelder¹ recognized that one effective strategy for numerically integrating stiff systems of ODEs was to solve the equations implicitly or, alternatively, to evaluate the chemical source terms at time level $n+1$. For problems involving PDEs several authors^{2,3} have described methods where terms involving spatial gradients are treated explicitly and the chemical source terms are evaluated implicitly (point-implicit methods). These studies, however, were

limited to one spatial dimension. In this article, these ideas are extended to multiple space dimensions, and it will be shown that these techniques are a special case of a general time scale preconditioner. Point-implicit techniques have important advantages over both explicit and fully implicit methods. A more complete discussion and analysis of the research may be found in Ref. 4.

II. Governing Equations

The conservation equations governing viscous laminar two-dimensional flows with chemical reaction can be written as

$$\frac{\partial U}{\partial t} + \frac{\partial F}{\partial x} + \frac{\partial G}{\partial y} + H = 0 \quad (2)$$

where U , F , G and H are,

$$U = \begin{bmatrix} \rho \\ \rho u \\ \rho v \\ \rho E \\ \rho Y_k \end{bmatrix} \quad F = \begin{bmatrix} \rho u \\ \rho u^2 + \sigma_{xx} \\ \rho uv + \tau_{xy} \\ \rho Eu + u\sigma_{xx} + v\tau_{yx} + q_x \\ \rho Y_k u - \Gamma Y_{kx} \end{bmatrix}$$

$$G = \begin{bmatrix} \rho v \\ \rho uv + \tau_{yx} \\ \rho v^2 + \sigma_{yy} \\ \rho Ev + v\sigma_{yy} + u\tau_{xy} + q_y \\ \rho Y_k v - \Gamma Y_{ky} \end{bmatrix} \quad H = \begin{bmatrix} 0 \\ 0 \\ 0 \\ 0 \\ -\dot{w}_k \end{bmatrix} \quad (3)$$

where Y_k is the k th species density fraction and \dot{w}_k is the k th species source term. The symbols ρ , u , v , T , p , t , x , and y represent the density, x velocity component, y velocity component, static pressure, time, x spatial variable, and y spatial variable. The various quantities can be written as

$$\sigma_{xx} = p - \lambda(u_x + v_y) - 2\mu u_x \quad (4)$$

Presented as Paper 85-0331 at the AIAA 23rd Aerospace Sciences Meeting, Reno, NV, Jan. 1985; received April 7, 1986; revision received June 10, 1987. Copyright © American Institute of Aeronautics and Astronautics, Inc., 1987. All rights reserved.

*Research Assistant, currently at Boeing Commercial Airplane Co., Seattle, VA.

†Professor, Department of Aeronautics and Astronautics. Fellow AIAA.

$$\tau_{xy} = -\mu(u_y + v_x) - \tau_{yx} \quad (5)$$

$$\sigma_{yy} = p - \lambda(u_x + v_y) - 2\mu v_y \quad (6)$$

$$q_x = -\kappa \frac{\partial T}{\partial x} - \sum \frac{\mu}{Pr} Hf_k \frac{\partial Y_k}{\partial x} \quad (7)$$

$$q_y = -\kappa \frac{\partial T}{\partial y} - \sum \frac{\mu}{Pr} Hf_k \frac{\partial Y_k}{\partial y} \quad (8)$$

$$\lambda = -\frac{2}{3}\mu \quad (9)$$

$$\kappa = \text{thermal conductivity} \quad (10)$$

$$\Gamma = \frac{\mu}{Sc} = \frac{\mu}{Pr} (Le = 1) \quad (11)$$

where Pr , Sc , and Le are the Prandtl, Schmidt, and Lewis numbers, respectively. Finally, to close the equation set, the total energy and the equation of state are given as

$$E = \sum_k Y_k \int_0^T C_{v,k} dT + \frac{u^2 + v^2}{2} + \sum_k H_{f,k} Y_k \quad (12)$$

$$P = \frac{\rho R^0 T}{Aw} \quad (13)$$

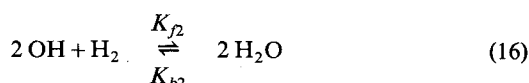
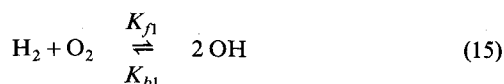
where $H_{f,k}$ is heat of formation for species k , R^0 is the universal gas constant, Aw is the molecular weight, Ns is the number of species, and k varies from 1 to $Ns-1$.

The laminar viscosity is calculated from Sutherland's law,

$$\mu_{\text{laminar}} = \frac{1.458 \times 10^{-6} T^{3/2}}{(T + 110.33)} \text{ kg/m-s} \quad (14)$$

III. H₂-Air Combustion Model

The H₂-air combustion model used in this study was proposed by Rogers and Chinitz⁵ in 1982. The model was developed to represent H₂-air combustion kinetics in a scram-jet combustor with as few reaction steps and species as possible. The model consists of the following two steps:



where the forward reaction rate constants K_{f1} and K_{f2} are given by

$$K_{fi} = A_i(\phi) T^{N_i} \exp^{-E_i/R^0 T} \quad (17)$$

where $A_i(\phi)$ is a function of the equivalence ratio ϕ . ϕ is defined as the fuel-to-air ratio divided by the stoichiometric fuel-to-air ratio. Values of the parameters used in this model are

$$A_1(\phi) = (8.917\phi + (31.433/\phi) - 28.950) 10^{47} \text{ cm}^3/\text{mole-s} \quad (18a)$$

$$A_2(\phi) = (2.000 + (1.333/\phi) - 0.833\phi) 10^{64} \text{ cm}^6/\text{mole}^2\text{-s} \quad (18b)$$

$$E_1 = 4865 \text{ cal/mole}$$

$$E_2 = 42,000 \text{ cal/mole}$$

$$N_1 = -10$$

$$N_2 = -13$$

$$R^0 = 1.987 \text{ cal/mole-K}$$

The backward reaction rates are given by

$$K_{b1} = K_{f1}/K_{eq1} \quad (19)$$

and

$$K_{b2} = K_{f2}/K_{eq2} \quad (20)$$

where K_{eq1} and K_{eq2} are the equilibrium constants for each reaction.

The model is valid for temperatures between 1000°K and 2000°K and equivalence ratios between 0.1 and 2.0. Because the chemistry model is not valid below a temperature of 1000°K, an ignition temperature must be specified. In this study the ignition temperature is equal to 1000°K, unless otherwise specified. The reaction rates for the various species conservation equations can be written as

$$\dot{w}_k = \dot{C}_k A w_k \quad (21)$$

where the various \dot{C}_k (mole/cm³-s) for the Rogers/Chinitz model are

$$\dot{C}_{\text{O}_2} = [-K_{f1} C_{\text{H}_2} C_{\text{O}_2} + K_{b1} (C_{\text{OH}})^2] \quad (22)$$

$$\dot{C}_{\text{H}_2\text{O}} = 2[K_{f2} C_{\text{H}_2} (C_{\text{OH}})^2 - K_{b2} (C_{\text{H}_2\text{O}})^2] \quad (23)$$

$$\dot{C}_{\text{H}_2} = (\dot{C}_{\text{O}_2} - \frac{1}{2} \dot{C}_{\text{H}_2\text{O}}) \quad (24)$$

$$\dot{C}_{\text{OH}} = -(2\dot{C}_{\text{O}_2} + \dot{C}_{\text{H}_2\text{O}}) \quad (25)$$

where $A w_k$ is the k th species molecular weight and the C 's are related to the Y 's through the following equation

$$C_k = \rho Y_k / A w_k \quad (26)$$

Finally, to close the equation set, a relation can be written for the sum of the species density fractions, i.e.,

$$Y_{\text{H}_2} + Y_{\text{O}_2} + Y_{\text{OH}} + Y_{\text{H}_2\text{O}} + Y_{\text{N}_2} = 1 \quad (27)$$

N_2 is present in the calculations but is assumed to be inert.

IV. Time Scale Preconditioning

If only the steady-state solution is desired, then the time history can be modified to remove the stiffness associated with the chemical time scales. Figure 1 schematically shows the paths taken in real time by a typical fluid and species quantity from an initial state to a final (steady) state. The figure shows that the species quantity undergoes a rapid change whereas the fluid quantity evolves much more slowly. It is this great disparity in the slopes of the two curves which is responsible for the stiffness in the problem. If, as shown in Fig. 2, the two quantities can be advanced together in pseudotime, then the fast processes which require small time steps would not hold up the slower processes which could be marched at larger time steps. This can be accomplished by modifying Eq. (2) to reflect this desired pseudotime behavior by rewriting it as

$$S \frac{\partial U}{\partial t} = -\frac{\partial F}{\partial x} - \frac{\partial G}{\partial y} - H \quad (28)$$

where S is a preconditioning matrix whose purpose is to normalize the various time scales to be of the same order. The

pseudotime history of the state quantities given by Eq. (28) might be very different from those given by Eq. (2), but both satisfy the same steady-state equation. If S is constructed correctly, the chemical time scales can be made approximately equal to the fluid time scales and the chemical stiffness can be removed from the problem. The scaling matrix could have a variety of forms, i.e., diagonal, triangular, full, etc. In the next section, we will consider what the elements of the scaling matrix should look like and how they can be constructed.

The method can be made time accurate by choosing numerical time steps small enough to reduce the error at any time step to some acceptable level. One way to do this is to set the numerical time step equal to some fraction of the time scale of the transient process of interest. The method can also be made time accurate simply by choosing S to be the identity matrix. It turns out that the numerical method can be coded to handle both time-accurate or pseudotime calculations with only minor changes to the code structure. However, in the present work, only steady-state calculations have been performed.

For inviscid and viscous flows without chemistry, the system of discrete finite-volume equations representing Eq. (2) are usually stiff.⁶ This stiffness arises from large variations in the cell size throughout the computational domain. From the numerical stability requirements for explicit methods, the allowable computational time step Δt in each cell is directly proportional to the cell size and therefore can vary by orders of magnitude over the domain. If the minimum value of Δt over the domain is used, the calculations are time accurate but converge very slowly to a steady state. If the allowable value of Δt is used for each cell (local time stepping), however, convergence to a steady state is greatly accelerated. It will be seen that the preconditioning introduced in this section effectively uses a different time step for the fluids (mass, momentum, and energy) and chemical (species) equations. This, together with local time stepping, greatly improves convergence to steady state for chemically reacting flow problems.

V. Derivation of the Scaling Matrix

As previously mentioned, the S matrix can take on a variety of forms. The form of the S matrix, and specifically what the matrix elements should contain, is now considered. If the time stiffness is to be removed from the problem, then the matrix S should in some way contain the chemical time scale. The desired time scale character can be seen by considering the species equation without the convective term, i.e.,

$$\frac{dU_Y}{dt} = -H = -\frac{kU_Y}{\rho} \quad (29)$$

Integrating this equation yields

$$U_Y = U_Y^0 e^{-kt/\rho} = U_Y^0 \exp^{-t/\tau_{\text{chem}}} \quad (30)$$

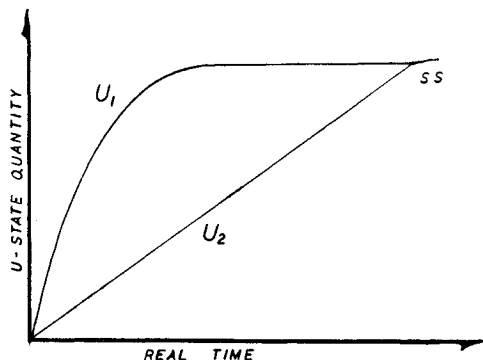


Fig. 1 Real time behavior of a typical species (U_1) and fluid (U_2) quantity.

where $\tau_{\text{chem}} = \rho/k$. Thus, we see that the U_Y evolution is dependent on the chemical time scale τ_{chem} through the exponential term. If H is differentiated with respect to U_Y as

$$\frac{\partial H}{\partial U_Y} = \frac{k}{\rho} = \frac{1}{\tau_{\text{chem}}} \quad (31)$$

we find that this derivative is equal to the inverse of the chemical time scale, τ_{chem} . This would suggest that the matrix S should contain elements like $\partial H/\partial U$. It should be pointed out that the derivative $\partial H/\partial U$ for a system of equations becomes a Jacobian matrix.

The point implicit method discussed in the introduction can be written as

$$\frac{U^{n+1} - U^n}{\Delta t} = -\left(\frac{\partial F}{\partial x} + \frac{\partial G}{\partial Y}\right)^n - H^{n+1} \quad (32)$$

where U , F , G , and H are given in Eq. (3). To solve this equation H^{n+1} can be linearized using the Newton method

$$H^{n+1} = H^n + \left(\frac{\partial H}{\partial U}\right)^n \Delta U + O(\Delta U^2) \quad (33)$$

where $\Delta U = U^{n+1} - U^n$. Substituting Eq. (33) into Eq. (32) yields

$$\begin{aligned} \frac{U^{n+1} - U^n}{\Delta t} = & -\left(\frac{\partial F}{\partial x} + \frac{\partial G}{\partial Y}\right)^n \\ & - \left[H^n + \left(\frac{\partial H}{\partial U}\right)^n (U^{n+1} - U^n) \right] \end{aligned} \quad (34)$$

which can be rewritten as

$$PI \left(\frac{U^{n+1} - U^n}{\Delta t} \right) = -\left(\frac{\partial F}{\partial x} + \frac{\partial G}{\partial y}\right)^n - H^n \quad (35)$$

where the matrix PI is equal to

$$PI = \left[I + \Delta t \left(\frac{\partial H}{\partial U} \right)^n \right] \equiv [I + \Delta t A] \quad (36)$$

The matrix elements $A_{ij} = \partial H_i / \partial U_j$ are inversely proportional to the various time scales considered necessary to rescale the equations in time. Comparing Eq. (36) with Eq. (28), we see that the matrix PI is a possible preconditioner. It is important to point out that this matrix has dimensions equal to the number of governing equations and not to the number of spatial grid points. It is small and easy to invert directly. Thus, the implicit treatment of the chemical source terms leads to one possible form of the desired scaling matrix.

Another type of preconditioner considered was to choose an S matrix containing only diagonal elements. With only diagonal elements, U^{n+1} can be obtained directly without the need to invert the S matrix. As a result, some savings in computational work per iteration could be realized. Dropping the off-diagonal terms, however, leads to inaccuracies in correctly time scaling the equations. If the inaccuracies are large, then the scheme will tend to be numerically unstable. Only a limited investigation was made with this type of preconditioner. The results indicate that with diagonal terms of the form

$$1 + 2\Delta t \frac{\partial H_k}{\partial U_k} \quad (37)$$

convergence was obtained in approximately twice as many iterations compared to the full point-implicit preconditioner. It is possible, although not shown, that, with enough species, the diagonal preconditioner could become more computa-

tionally efficient than the full point-implicit preconditioner. No attempt was made to determine where the crossover might occur or even if one exists. In addition it might be possible to find approximations for the Jacobian derivatives which could reduce the computational work required to compute the S matrix. For example, Pratt⁷ has suggested using exponentials to approximate the Jacobian derivatives.

Finally, another technique was explored which possesses some of the attributes of preconditioning the equations to effectively time scale them. This method will be referred to as Local Time Cycling (LTC). In the LTC method the equations are solved explicitly but are numerically updated only in certain regions of the computational domain, depending upon the total accumulated time for each particular cell. If, at the beginning of the calculation, all cells begin with zero accumulated time, then the total accumulated time is the sum of all the numerical time steps that the equations in a given cell have been advanced at since the beginning of the calculation. The LTC method would prove useful if the equations are stiff in part of the domain. The stiffness could limit the numerical time step taken in these cells and hold back the longer time scale physics there compared to the rest of the domain. The method is implemented as follows. The first step consists of one explicit iteration of all the equations over the complete global domain, i.e., one global iteration. If, after the global iteration, the accumulated time in any given cell is less than in its neighboring cells, then the equations in that particular cell are integrated in time until their accumulated time equals the accumulated time in the neighboring cells. It might be necessary to advance the equations in a given cell several times, local time cycling, and repeat the process every global iteration. The method has the advantage that it does not require the evaluation of the Jacobian derivatives. There is additional computational work, however, which is associated with locally solving the equations and in determining which parts of the domain should be local time cycled. For the examples considered in this article, the LTC method proved less efficient than the full point-implicit preconditioner. However, if the number of species becomes large, the LTC method could prove useful.

VI. Interpretation of Time Scaling

The scaling matrix S derived in the previous section can be shown to possess the desired character needed to remove the chemical time scale stiffness. To understand this process, consider the O_2 dissociation reaction



for a compressible flow in a variable area duct of cross-sectional area A . Using the quasi-one-dimensional assumption and assuming inviscid flow, the system of equations to be solved becomes

$$\frac{\partial U}{\partial t} = -\frac{\partial F}{\partial x} - H \quad (39)$$

where

$$U = \begin{bmatrix} \rho A \\ \rho u A \\ \rho E A \\ \rho Y_{O_2} A \end{bmatrix} \quad F = \begin{bmatrix} \rho u A \\ \rho u^2 A + p A \\ \rho u H A \\ \rho u Y_{O_2} A \end{bmatrix} \quad H = \begin{bmatrix} 0 \\ -p dA/dx \\ 0 \\ -\dot{w}_{O_2} A \end{bmatrix} \quad (40)$$

To simplify the example, only a forward reaction rate is considered and

$$H_{O_2} = A \dot{w}_{O_2} = A k Y_{O_2} = k U_{O_2} / \rho = U_{O_2} / \tau_{chem} \quad (41)$$

The effective time steps used by each equation within the system of equations can be illustrated by using the point-implicit MacCormack method.⁸ The scaling matrix S for the quasi-one-dimensional problem reduces to the following,

$$S = \begin{bmatrix} 1 & 0 & 0 & 0 \\ 0 & 1 & 0 & 0 \\ 0 & 0 & 1 & 0 \\ \Delta t \partial H_{O_2} / \partial U_\rho & 0 & 0 & 1 + \Delta t \partial H_{O_2} / \partial U_{O_2} \end{bmatrix} \quad (42)$$

Note that only the chemical source terms, \dot{w} , of the vector H are treated implicitly. The point implicit predictor equation for the continuity equation can be written as

$$\Delta U_\rho = \Delta t [\text{Res}]_\rho^n \quad (43)$$

where

$$[\text{Res}]_\rho^n = -\frac{(F_{\rho i+1}^n - F_{\rho i}^n)}{\Delta x} \quad (44)$$

ΔU_ρ represents the change in ρA and Δt is the numerical time step. In a similar way an expression for the change in $\rho Y_{O_2} A$ is given by

$$\Delta U_{O_2} = \frac{\Delta t}{1 + \Delta t \partial H_{O_2} / \partial U_{O_2}} \left([\text{Res}]_{O_2}^n - \frac{\partial H_{O_2}}{\partial U_\rho} \Delta U_\rho \right) \quad (45)$$

$$[\text{Res}]_{O_2}^n = -\frac{(F_{O_2 i+1}^n - F_{O_2 i}^n)}{\Delta x} - H_{O_2}^n \quad (46)$$

$$\Delta U_{O_2} = \frac{\Delta t}{1 + \Delta t / \tau_{chem}} \left([\text{Res}]_{O_2}^n - \frac{\partial H_{O_2}}{\partial U_\rho} \Delta U_\rho \right) \quad (47)$$

Now if we choose

$$\Delta t = \frac{\Delta x}{|U + a|} \equiv \tau_{fluid} \quad (48)$$

where a is the speed of sound, and if $\tau_{fluid} \gg \tau_{chem}$, i.e., the equations are stiff, then Eqs. (43) and (47) become

$$\Delta U_\rho = \tau_{fluid} [\text{Res}]_\rho^n \quad (49)$$

and

$$\Delta U_{O_2} \approx \tau_{chem} \left([\text{Res}]_{O_2}^n - \frac{\partial H_{O_2}}{\partial U_\rho} \Delta U_\rho \right) \quad (50)$$

For this simple example it can be seen that the time step used to advance the fluid dynamic variables is τ_{fluid} while that used to advance the species term is τ_{chem} . This achieves the goal illustrated in Fig. 2.

So far we have considered a reaction model with only a forward rate. If we include both the forward and backward rates and consider the situation where the convective terms are small compared to the chemical source terms, the conservation equation for O_2 can be written as

$$\Delta U_{O_2} \approx -\tau_{chem} H_{O_2}^n = \tau_{chem} \left(\frac{U_{eq} - U_{O_2}^n}{\tau_{chem}} \right) = U_{eq} - U_{O_2}^n \quad (51)$$

where U_{eq} is the local equilibrium value of U . In this case U is always advanced to its local equilibrium value over one iteration. If the convective term becomes important later on in the calculation, then U is advanced at the local chemical reaction

time scale. Thus, in general, time scaling the equations is equivalent to advancing each state quantity at its own characteristic rate.

If numerical time steps taken are large compared to the smallest value of τ_{chem} , then the solution is no longer time accurate. But, as we will see in the next section, the convergence rate is dramatically improved. The time scaling method can be made time accurate by reducing the numerical time step everywhere to the physical time scales of interest.

The preconditioning procedure is applied only to those regions of the domain where the stiffness level is greater than approximately one. This implies that, wherever the stiffness level is greater than one, the point-implicit preconditioner is used, and wherever the stiffness level is less than one, no preconditioner is used.

VII. Results

Four different calculations were performed to demonstrate the capability and efficiency of the method for chemically reacting flows. These calculations include one- and two-dimensional inviscid and viscous examples. The one-dimensional examples were computed using a preconditioned version of the explicit MacCormack⁸ scheme (Appendix A). The two-dimensional examples were computed using a preconditioned version of the Jameson, Schmidt, and Turkel⁹ scheme (Appendix A). The use of two different schemes was a result of the historical development of the present research rather than any difficulty encountered with either algorithm. It serves to illustrate that the suggested approach is generally applicable to all explicit algorithms.

The first application of the preconditioning method was to predict the steady state of a simple diatomic dissociation problem. The coefficients used in the chemistry model do not necessarily represent real oxygen dissociation, but were chosen to produce the desired challenge of an extremely stiff equation set. The inflow conditions and chemistry model rate constants for this problem are given in Table 1. A quasi-one-dimensional converging-diverging nozzle configuration was adopted. The geometry was chosen to produce a high-temperature region in the flow field where the dissociation could occur. Figure 3 shows the the distribution of O_2 and O through the nozzle. Dissociation occurs over a very thin reaction region. Figure 4 shows the corresponding distributions of the nondimensional fluid and O_2 reaction rate time scales. The maximum stiffness parameter reached is approximately 1000. The convergence histories for this problem, shown in Fig. 5, compare the number of iterations required to reach a steady state defined as a five-order-of-magnitude reduction in the residual. The four cases shown represent setting 1) Δt everywhere equal to the minimum Δt (time accurate solution, 2) keeping the Courant, Friedrichs, and Lewy (CFL) number constant (local time stepping), 3) applying the time preconditioner with the constant CFL condition, and 4) method 3 plus a multigrid method described in Appendix B. The first method

required an estimated 10^6 iterations, the second method required 10^5 iterations, while the third method required only 300 iterations. The nonreacting problem, $\dot{w}=0$, required approximately 200 iterations to reach steady state. Case 4 required approximately 100 iterations to reach convergence. Varying the stiffness two orders of magnitude in either direction did not change the number of iterations needed for the preconditioned method to converge. The number of iterations needed for the first two methods was found to be directly proportional to the level of stiffness. Thus, the time scale preconditioner effectively removes the limitations caused by the chemical time scale.

Table 1 Data for O_2 dissociation in converging-diverging nozzle

Properties	Values	Dimensions
P_∞	6.6×10^4	N/m ²
T_∞	1200	°K
M_∞	6	
c_{pO_2}	1040	J/kg °K
c_{pO}	780	J/kg °K
c_{vO_2}	600	J/kg °K
c_{vO}	500	J/kg °K
Hf_{O_2}	0	J/kg
Hf_O	1.0×10^5	J/kg
L	0.213	m
$w = AT^{-B}e^{-C/T}$		
A	1.0×10^{14}	
B	-1	
C	80	
Grid	129	
CFL	0.9	

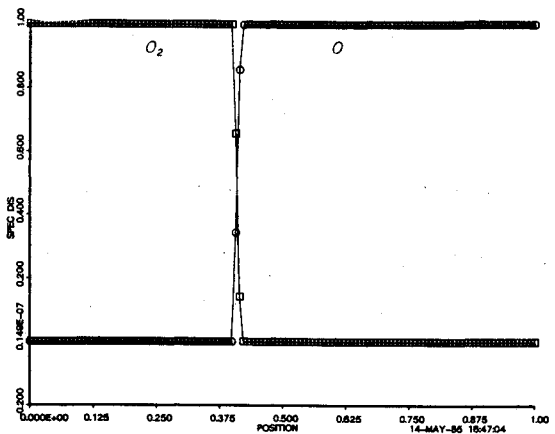


Fig. 3 O_2 and O species plot for O_2 dissociation in a converging-diverging nozzle.

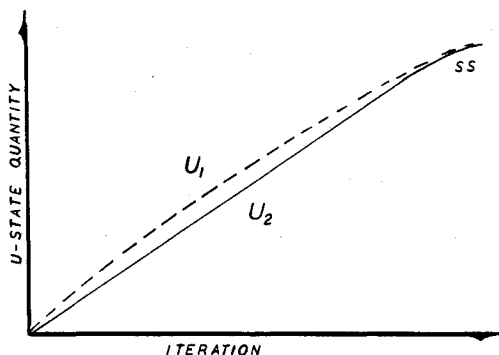


Fig. 2 Pseudo time behavior of a typical species (U_1) and fluid (U_2) quantity.

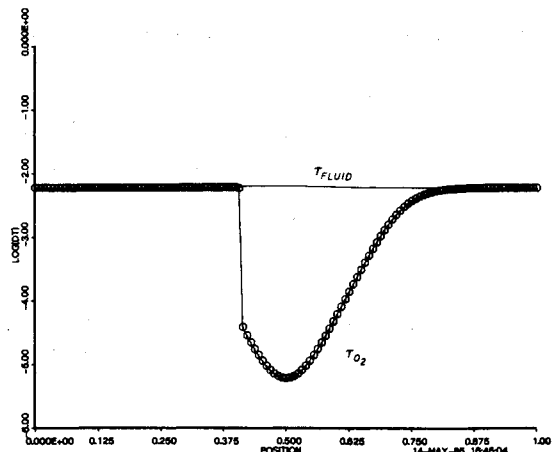


Fig. 4 Reacting time scale plot for O_2 dissociation in a converging-diverging nozzle.

The second example to be considered is H_2 -air combustion in a simple diverging nozzle. The quasi-one-dimensional Euler equations with finite rate chemistry are solved for parameters given in Tables 2 and 3. The distribution of the H_2O and OH density fractions is shown in Fig. 6. The density fraction of OH undergoes a large step change in the first cell, indicating that the OH production reaction is very fast. The H_2O production rate, however, is much slower as indicated by the gradual change in its slope. A comparison between the computed H_2O density fraction and another calculation performed by Drummond shows excellent agreement. (The results were obtained in a personal communication from Phil Drummond, NASA Langley Research Center, and were calculated using the methods of Ref. 10.) For this problem the maximum stiffness reached is approximately 10^6 .

In the third example, the preconditioning technique is applied to the two-dimensional Euler equation with the Rogers and Chinitz H_2 -air chemistry model. A premixed hydrogen-air stream at Mach number 2.5 is directed at a 10 deg compression ramp. The temperature rise across the oblique shock wave generated by the ramp can initiate and stabilize a chemical reaction under the right circumstances (a supersonic flame holder). For the calculation, properties at the inflow boundary were held at their freestream levels. At the supersonic downstream boundary, conditions were extrapolated from the interior. The top and bottom boundaries were modeled as slip boundaries. Figure 7 shows the H_2O density fraction contours for property values given in Tables 2 and 3. For this case, ignition occurs at the oblique wave and the corresponding heat release moves the shock wave upstream somewhat from its nonreacting position. Further discussion of this example and other cases may be found in Refs. 4 and 11.

For the final example, the method is applied to laminar reacting flow over a rearward facing step for the property values given in Tables 2 and 3. At the inflow boundary, all quantities were specified including a Blasius boundary-layer

profile with a thickness the same order as the step height. The solid lower wall was modeled as a adiabatic, noncatalytic,

Table 3 Chemistry data for H_2 -air calculations (NASA SP-3001)

Property	Dimensions	Value
C_{pH_2O}	J/kg $^{\circ}$ K	17,160
C_{pOH}	J/kg $^{\circ}$ K	1181
C_{pH_2}	J/kg $^{\circ}$ K	2854
C_{pO_2}	J/kg $^{\circ}$ K	2041
C_{pN_2}	J/kg $^{\circ}$ K	1285
C_{vH_2O}	J/kg $^{\circ}$ K	17,160
C_{vOH}	J/kg $^{\circ}$ K	1181
C_{vH_2}	J/kg $^{\circ}$ K	2854
C_{vO_2}	J/kg $^{\circ}$ K	2041
C_{vN_2}	J/kg $^{\circ}$ K	1285
Hf_{H_2O}	J/kg	-1.44×10^7
Hf_{OH}	J/kg	2.3×10^6
Hf_{H_2}	J/kg	0
Hf_{O_2}	J/kg	0
Hf_{N_2}	J/kg	0

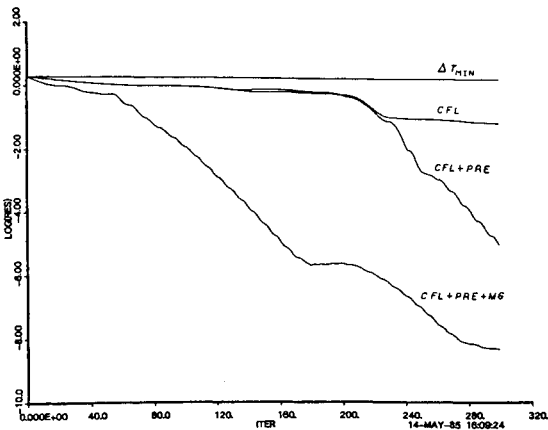


Fig. 5 Reacting convergence history plot for O_2 dissociation in a converging-diverging nozzle.

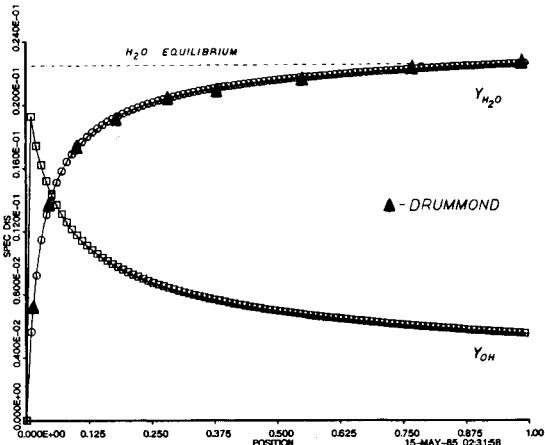


Fig. 6 H_2O and OH species distribution for a premixed H_2 -air reaction in a diverging duct.

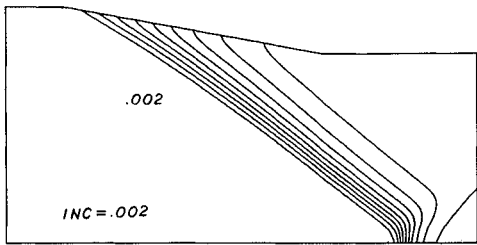


Fig. 7 H_2O density fraction contour plot for an $M=2.5$ inviscid premixed H_2 -air ($\phi=0.1$) flow past a 10° compression ramp.

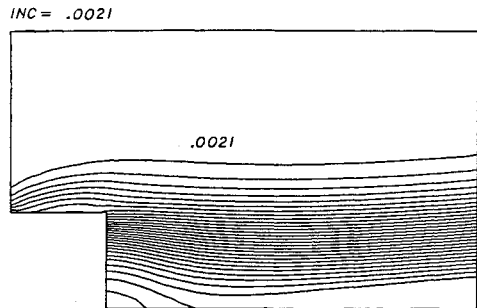


Fig. 8 H_2O density fraction contour plot for an $M=2.0$ laminar premixed H_2 -air ($\phi=0.5$) flow over a rearward facing step.

Table 2 Data for H_2 -air calculations

Property	Dimensions	Values	
		2-D Ramp	2-D Step
P_{∞}	N/m 2	1.0×10^5	1.0×10^5
T	$^{\circ}$ K	900	900
T_{ignition}	$^{\circ}$ K	1000	1300
ϕ		0.1	0.5
M_{∞}		2.5	2.0
U_{∞}	m/s	1500	1200
V_{∞}	m/s	0	0
Re_H			230,000
Pr			1.0

nonslip surface. The upper boundary is a symmetry plane, and all quantities were extrapolated at the outflow boundary. Validation of the basic nonreacting numerical method is contained in Ref. 4. Figure 8 shows the H₂O density fraction contours. Ignition occurs in the boundary layer ahead of the step, and a total H₂O mass fraction of about 5.9% is formed by the reaction. Further discussion of this and other examples is contained in Refs. 4 and 11.

VIII. Conclusions

Several conclusions can be drawn from this study:

1) A preconditioning technique is presented which accelerates the convergence rate of multidimensional fluid problems involving finite rate chemistry.

2) The point implicit scheme, i.e., treating the convective and diffusion terms explicitly and the chemical source terms implicitly, leads to a preconditioner which effectively removes the chemical time scale limitations of explicit methods.

3) Both the MacCormack and the Jameson, Schmidt, and Turkel methods have been shown to work well with the preconditioning technique.

4) The preconditioning technique has been applied to a realistic H₂-air chemistry model and used successfully to model nontrivial chemical reacting flows.

5) The results show that with preconditioning of the equations, convergence to steady state can be achieved in approximately the same number of iterations as that needed to solve the nonreacting problem.

Appendix A

MacCormack's 1969 explicit two-step, second-order-accurate in both space- and time-finite difference method is given as⁸

$$\Delta \bar{U}^* = -\Delta t \left(\frac{(\bar{F}_{i+1}^n - \bar{F}_i^n)}{\Delta x} + \bar{H}_i^n \right)$$

$$\Delta \bar{U}^1 = -\Delta t \left(\frac{(\bar{F}_i^* - \bar{F}_{i-1}^*)}{\Delta x} + \bar{H}_i^* \right)$$

where

$$\bar{U}_i^{n+1} = \frac{1}{2} (\bar{U}_i^1 + \bar{U}_i^*)$$

and

$$\Delta \bar{U}^* = \bar{U}_i^* - \bar{U}_i^n$$

$$\Delta \bar{U}^1 = \bar{U}_i^1 - \bar{U}_i^n$$

The scheme is stable for CFL ≤ 1 .

The point implicit form of the MacCormack 1969 scheme is given as

$$\bar{S} \bar{M} \Delta \bar{U}^* = -\Delta t \left(\frac{(\bar{F}_{i+1}^n - \bar{F}_i^n)}{\Delta x} + \bar{H}_i^n \right)$$

$$\bar{S} \bar{M} \Delta \bar{U}^1 = -\Delta t \left(\frac{(\bar{F}_i^* - \bar{F}_{i-1}^*)}{\Delta x} + \bar{H}_i^* \right)$$

and

$$\bar{U}_i^{n+1} = \frac{1}{2} (\bar{U}_i^1 + \bar{U}_i^*)$$

where

$$\Delta \bar{U}^* = \bar{U}_i^* - \bar{U}_i^n$$

$$\Delta \bar{U}^1 = \bar{U}_i^1 - \bar{U}_i^n$$

where $\bar{S} \bar{M}$ is the preconditioning matrix given below.

The explicit Jameson, Schmidt, and Turkel finite-volume, multistage time-stepping method⁹ can be described as follows. First the residual, R , is defined to be

$$R_{ij} = \frac{1}{S_{ij}} (Q_{ij} - D_{ij})$$

where Q_{ij} is the net flux out of the cell i,j plus the contributions due to any source terms in cell i,j . S_{ij} is the cell area and D_{ij} is an added dissipation term. Next the scheme can be written as

$$U^{(0)} = U^n$$

$$U^{(1)} = U^{(0)} - \alpha_1 \Delta t R (U^{(0)})$$

$$U^{(2)} = U^{(0)} - \alpha_2 \Delta t R (U^{(1)})$$

$$U^{(3)} = U^{(0)} - \alpha_3 \Delta t R (U^{(2)})$$

$$U^{(4)} = U^{(0)} - \alpha_4 \Delta t R (U^{(3)})$$

$$U^{n+1} = U^{(4)}$$

where the integrations constants $\alpha_1, \alpha_2, \alpha_3$, and α_4 are 1/4, 1/3, 1/2, and 1, respectively. The scheme is stable for CFL's equal to or less than $2\sqrt{2}$.

The point implicit version of this scheme can be written as

$$\bar{U}^0 = \bar{U}^n$$

$$\bar{S} \bar{J}^0 (\bar{U}^1 - \bar{U}^0) = -\alpha_1 \Delta t \bar{R}^0$$

$$\bar{S} \bar{J}^1 (\bar{U}^2 - \bar{U}^0) = -\alpha_2 \Delta t \bar{R}^1$$

$$\bar{S} \bar{J}^2 (\bar{U}^3 - \bar{U}^0) = -\alpha_3 \Delta t \bar{R}^2$$

$$\bar{S} \bar{J}^3 (\bar{U}^4 - \bar{U}^0) = -\alpha_4 \Delta t \bar{R}^3$$

$$\bar{U}^{n+1} = \bar{U}^4$$

where $\bar{S} \bar{J}$ represents the preconditioning matrix given in the following.

The preconditioning matrices for the point implicit MacCormack $\bar{S} \bar{M}$, Jameson $\bar{S} \bar{M}$, and Ni¹² $\bar{S} \bar{N}$ multiple schemes are given as

$$\bar{S} = \begin{bmatrix} 1 + A \Delta t \frac{\partial H_1}{\partial U_1} & + A \Delta t \frac{\partial H_1}{\partial U_2} & \dots & + A \Delta t \frac{\partial H_1}{\partial U_N} \\ + A \Delta t \frac{\partial H_2}{\partial U_1} & 1 + A \Delta t \frac{\partial H_2}{\partial U_2} & & \vdots \\ \vdots & \vdots & \ddots & \vdots \\ + A \Delta t \frac{\partial H_N}{\partial U_1} & \dots & & 1 + A \Delta t \frac{\partial H_N}{\partial U_N} \end{bmatrix}$$

where $A = 1$ for the point-implicit version of the MacCormack scheme, $A = \alpha$ for the point-implicit version of the Jameson, Schmidt, and Turkel scheme, and $A = 1/2$ for the point implicit Ni scheme. Note the $\partial H / \partial U$'s for the point implicit Ni scheme are based on fine grid averages of $\partial H / \partial U$.

Appendix B

Acceleration of the compressible Euler and Navier-Stokes equations using multigrid methods has been reported by several authors.¹²⁻¹⁵ A limited investigation was conducted to ascertain if multigrid methods could be extended to the finite-rate chemistry problems under consideration here. Studies for the one-dimensional equations using Ni's¹² method were suc-

cessful and are reported here. To the best of the authors' knowledge this represents the first successful application of multigrid methods to this class of problem. The basic Ni method for the Euler equations is reviewed before presenting the extensions to include the chemical source terms.

Basic Ni Multiple Grid Method

Starting with the one-dimensional Euler equations

$$\frac{\partial U}{\partial t} + \frac{\partial F}{\partial x} = 0 \quad (B1)$$

the Ni method can be described as having five steps.

Step 1

The fine grid correction δU_I is computed (see Fig. 9 for notation).

$$\delta U_I = [(\delta U)_A + (\delta U)_B] \quad (B2)$$

where

$$(\delta U)_A = \frac{1}{2} \left(\Delta U_A + \frac{\Delta t}{\Delta x} \Delta F_A \right) \quad (B3)$$

$$(\delta U)_B = \frac{1}{2} \left(\Delta U_B - \frac{\Delta t}{\Delta x} \Delta F_B \right) \quad (B4)$$

$$\Delta U_A = \frac{\Delta t}{\Delta x} (F_{I-1}^n - F_I^n) \quad (B5)$$

$$\Delta U_B = \frac{\Delta t}{\Delta x} (F_I^n - F_{I+1}^n) \quad (B6)$$

$$\Delta F = \left(\frac{\partial F}{\partial U} \right) \Delta U \quad (B7)$$

Step 2

A coarse grid is constructed by removing every other fine grid cell (Fig.9) and the corrections from the fine (h) grid are transferred to the coarse grid ($2h$) by

$$\Delta U^{2h} = T_h^{2h} \delta U^h \quad (B8)$$

where T is an operator which transfers to each control volume of the coarse grid the correction δU^h of the centered fine-grid point.

Step 3

In this step the coarse-grid acceleration is performed to propagate fine-grid changes more quickly out of the domain. The coarse-grid correction is computed as follows:

$$\delta U_i^{2h} = [(\delta U)_a^{2h} + (\delta U)_b^{2h}] \quad (B9)$$

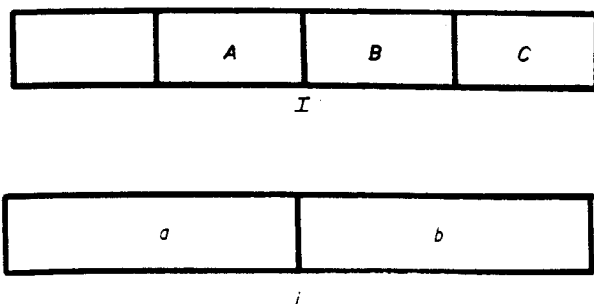


Fig. 9 Nomenclature for multigrid; top—fine cell, bottom—coarse cell.

$$(\delta U)_a^{2h} = \frac{1}{2} \left[\Delta U_a^{2h} + \left(\frac{\Delta t}{\Delta x} \right)^{2h} \Delta F_a^{2h} \right] \quad (B10)$$

$$(\delta U)_b^{2h} = \frac{1}{2} \left[\Delta U_b^{2h} - \left(\frac{\Delta t}{\Delta x} \right)^{2h} \Delta F_b^{2h} \right] \quad (B11)$$

where Eq. (B8) defines the ΔU values and Eq. (B7) is used for ΔF with $\partial F / \partial U$ evaluated at level h .

Step 4

The coarse grid corrections are interpolated back down to the finest level by

$$\delta U_I^{2h} = I_{2h}^h \delta U_I^{2h} \quad (B12)$$

where I_{2h}^h is a linear interpolation operator.

Step 5

The last step updates the state variables with the corrections from all grid levels by

$$U_I^{n+1} = U_I^n + \delta U_I^h + \delta U_I^{2h} + \delta U_I^{4h} + \dots + \delta U_I^{kh} \quad (B13)$$

where k is the coarsest level chosen. These five steps represent a single Ni multiple grid cycle.

Point Implicit Ni Multiple Grid Method

When the chemical source terms H are added to Eq. (B1), preconditioning of the equations used in steps 1 and 3 are required to remove the stiffness. In the present application, McCormack's method was used to compute the correction δU_I^h on the fine grid as reported in the first example. Following the suggestion of Johnson¹⁴ this was used in place of Ni's fine grid solver, but the Ni method was used for the coarse grid acceleration. Steps 2, 4, and 5 remain unchanged. The modifications required to step 3 are now given.

The inclusion of the chemical source terms modifies Eq. (B9), (B10), and (B11) to

$$(\delta U)_i^{2h} = (\delta U)_a^{2h} + (\delta U)_b^{2h} \quad (B14)$$

$$(\delta U)_a^{2h} = \frac{1}{2} \left[\Delta \bar{U}_a^{2h} + \left(\frac{\Delta t}{\Delta x} \right)^{2h} \Delta \bar{F}_a^{2h} + \left(\frac{\Delta t}{2} \right)^{2h} \Delta \bar{H}_a^{2h} \right] \quad (B15)$$

$$(\delta U)_b^{2h} = \frac{1}{2} \left[\Delta \bar{U}_b^{2h} - \left(\frac{\Delta t}{\Delta x} \right)^{2h} \Delta \bar{F}_b^{2h} - \left(\frac{\Delta t}{2} \right)^{2h} \Delta \bar{H}_b^{2h} \right] \quad (B16)$$

where

$$\Delta \bar{F}^{2h} = \left(\frac{\partial \bar{F}}{\partial U} \right)^{2h} \Delta \bar{U}^{2h} \quad (B17)$$

$$\Delta \bar{H}^{2h} = \left(\frac{\partial H}{\partial U} \right)^{2h} \Delta \bar{U}^{2h} \quad (B18)$$

Now, since

$$\frac{\partial H}{\partial U} \propto \frac{1}{\tau_{\text{chem}}} \quad (B19)$$

[See Eq. (31)]; Eqs. (B15) and (B16) can be stiff if $\tau_{\text{chem}} \ll \tau_{\text{fluid}}$. Thus if the multiple grid procedure is to be utilized, these equations must be preconditioned, i.e., $\Delta \bar{H}^{2h}$ treated implicitly. The simplest formulation that seems to work best is to set the $\Delta \bar{U}^{2h}$ in the $\Delta \bar{H}^{2h}$ expression [Eq. (B18)] equal to $\delta \bar{U}^{2h}$, i.e.,

$$\Delta \bar{U}_a^{2h} = (\delta \bar{U})_a^{2h} \quad (B20a)$$

$$\Delta \bar{U}_b^{2h} = (\delta \bar{U})_b^{2h} \quad (\text{B20b})$$

It was found best not to recompute $\partial H/\partial U$ on the coarse grid levels, but instead to evaluate it by area averaging $\partial H/\partial U$ computed on the finest grid. For example, for cell b ($2h$ level)

$$\left(\frac{\partial H}{\partial U}\right)_b^{2h} = \left(\frac{\partial H}{\partial U}\right)_B^o \times \Lambda_x + \left(\frac{\partial H}{\partial U}\right)_C^h \times S_C / S_B + S_C \quad (\text{B21})$$

where S is the cell area. Basing $(\partial H/\partial U)^{2h}$ on the finest level is necessary as the chemical time scales, τ_{chem} , can be very sensitive to temperature. If $\partial H/\partial U$ was recomputed on each coarse level, the temperature used would be an average value over many fine cells. This average temperature could produce a very different chemical reaction behavior which would not be consistent with the fine grid predictions.

Thus, rewriting Eqs. (B15) and (B16) with the source term treated implicitly leads to

$$\overline{SN}(\delta \bar{U})_a^{2h} = \frac{1}{2} \left(\Delta \bar{U}_a^{2h} + \frac{\Delta t}{\Delta x} \Delta \bar{F}_a^{2h} \right) \quad (\text{B22a})$$

$$\overline{SN}(\delta \bar{U})_b^{2h} = \frac{1}{2} \left(\Delta \bar{U}_b^{2h} - \frac{\Delta t}{\Delta x} \Delta \bar{F}_b^{2h} \right) \quad (\text{B22b})$$

where \overline{SN} is given in Appendix A.

If the point-implicit version of MacCormack's scheme is used in conjunction with the point-implicit version of Ni's multiple grid scheme, convergence to steady state is achieved in 100 iterations for the dissociation problem discussed previously, Fig. 5. This represents a real computational work savings of approximately two. Three coarse grid levels were used in this problem. Note machine zero is reached here after the residual drops by approximately 10^{-7} .

It should be pointed out that the savings obtained are typical also of nonreacting flows obtained by the author.⁴ The computed distributions agree identically with those computed without the multiple grid. Based on this and other results, the number of iterations required for convergence appear to be independent of the stiffness associated with the chemical source terms. For more information the reader is referred to Ref. 4.

Acknowledgments

This research was supported by NASA Langley Research Center under Grant NAG-1-229 monitored by Dr. L. Beach

and Mr. G. Anderson. During the final editing of this manuscript, Ref. 16, which presents a similar method, was brought to the authors' attention.

References

- ¹Curtiss, C.F. and Hirschfelder, J.O., "Integration of Stiff Equations," *Proceedings of the National Academy of Sciences of the United States of America*, Vol. 38, 1952.
- ²Smoot, L.D., Hecker, W.C., and Williams, G.A., "Prediction of Propagating Methane-Air Flames," *Combustion and Flame*, Vol. 26, 1976.
- ³Otey, G.R. and Dwyer, H.A., "Numerical Study of the Interaction of Fast Chemistry and Diffusion," *AIAA Journal*, Vol. 17, June 1983, pp. 606-613.
- ⁴Bussing, T.R.A., "A Finite Volume Method for the Navier-Stokes Equations with Finite Rate Chemistry," Ph.D. Dissertation, Dept. of Aeronautics and Astronautics, Massachusetts Inst. of Technology, Cambridge, MA, Sept. 1985.
- ⁵Rogers, R.C. and Chinitz, W., "On the Use of a Global Hydrogen-Air Combustion Model in the Calculation of Turbulent Reacting Flows," AIAA Paper 82-0112, Jan. 1982.
- ⁶Eriksson, L.E. and Rizzi, A., "Analysis by Computer of the Convergence to Steady State of Discrete Approximations to the Euler Equations," AIAA Paper 83-1951-CP, July 1983.
- ⁷Pratt, D.T., "CREK-1D: A Computer Code for Transient, Gas-Phase Combustion Kinetics," *The Western States Section, The Combustion Institute*, April 1983.
- ⁸MacCormack, R.W., "The Effects of Viscosity on Hypervelocity Impact Cratering," AIAA Paper 69-345, May 1969.
- ⁹Jameson, A., Schmidt, W., and Turkel, E., "Numerical Solution of the Euler Equations by Finite Volume Methods Using Runge-Kutta Time-Stepping Scheme," AIAA Paper 81-1259, July 1981.
- ¹⁰Drummond, J.P., Hussaini, M.Y., and Zang, T., "Spectral Methods for Modeling Supersonic Chemically Reacting Flows," *AIAA Journal*, Vol. 24, Sept. 1986, pp. 1453-1460.
- ¹¹Bussing, T.R.A. and Murman, E.M., "Numerical Investigation of 2-Dimensional H_2 -Air Flame Holding over Ramps and Rearward Facing Steps," *Journal of Propulsion and Power*, Vol. 3, Sept.-Oct. 1987, pp. 448-454.
- ¹²Ni, R., "A Multiple-Grid Scheme for Solving the Euler Equations," *AIAA Journal*, Vol. 20, Nov. 1982, pp. 1565-1571.
- ¹³Jameson, A., "Solution of the Euler Equations for Two Dimensional Transonic Flow by a Multigrid Method," Princeton Univ. MAE Rept. 1613, June 1983.
- ¹⁴Johnson, G.M., "Multiple-Grid Acceleration of Lax-Wendroff Algorithms," NASA-TM-82843, 1982.
- ¹⁵Chima, R.V., "Analysis of Inviscid and Viscous Flows in Cascades with an Explicit Multiple-Grid Algorithm," AIAA Paper 84-1663, June 1984.
- ¹⁶Widhopf, G.F. and Victoria, K.J., "On the Solution of the Unsteady Navier-Stokes Equations Including Multicomponent Finite Rate Chemistry," *Computers and Fluids*, Vol. 1, 1973, pp. 159-184.